Zero kinetic energy-pulsed field ionization and resonance enhanced multiphoton ionization photoelectron spectroscopy: Ionization dynamics of Rydberg states in HBr

N. P. L. Wales, W. J. Buma, and C. A. de Lange
Laboratory for Physical Chemistry, University of Amsterdam, Nieuwe Achtergracht 127, 1018 WS Amsterdam, The Netherlands

H. Lefebvre-Brion
Laboratoire de Photophysique Moléculaire, Bât. 213, Université de Paris-Sud, 91405 Orsay Cedex, France

Kwanghsi Wang and V. McKoy
Arthur Amos Noyes Laboratory of Chemical Physics, California Institute of Technology, Pasadena, California 91125

(Received 11 December 1995; accepted 22 December 1995)

The results of rotationally resolved resonance enhanced multiphoton ionization photoelectron spectroscopy and zero kinetic energy-pulsed field ionization studies on HBr via various rotational levels of the $F\ ^1\Delta_2$ and $f\ ^3\Delta_2$ Rydberg states are reported. These studies lead to an accurate determination of the lowest ionization threshold as $94\,098.9 \pm 1\ \mathrm{cm}^{-1}$. Observed rotational and spin–orbit branching ratios are compared to the results of *ab initio* calculations. The differences between theory and experiment highlight the dominant role of rotational and spin–orbit interactions for the dynamic properties of the high-n Rydberg states involved in the pulsed field ionization process. © *1996 American Institute of Physics.* [S0021-9606(96)01712-2]

I. INTRODUCTION

The study of autoionizing Rydberg states located between the $X\ ^2\Pi_{3/2}$ and $^2\Pi_{1/2}$ spin–orbit components of the ground ionic state of the hydrogen halides has been a topic of considerable interest in recent years.[1–5] These states have attracted special attention because their description requires an angular momentum coupling scheme which changes from Hund's case (c) for low values of the principal quantum number n to Hund's case (e) for higher values.[6] Apart from their spectroscopic description, a detailed characterization of these states is also of utmost importance for a proper understanding of the appearance of zero kinetic energy-pulsed field ionization (ZEKE-PFI) spectra, which explicitly use the high-n Rydberg states converging upon rotational levels of the ionic states.[7]

In order to elucidate the spectroscopic and dynamic properties of such autoionizing Rydberg states in a reliable manner, one obviously requires a detailed knowledge of the ionic state spectroscopic constants, as well as an accurate determination of the ionization energy. Moreover, ideally one would like to study electronically similar molecules for which discrete–discrete and discrete–continuum interactions are distinctly different. In recent years HCl has been the subject of such extensive studies.[2,4,5] Spectroscopic parameters of its ionic states have been determined with high precision,[8] while the role of rotational and spin–orbit autoionization was highlighted in various ZEKE-PFI studies[9–11] in combination with resonance enhanced multiphoton ionization photoelectron spectroscopy (REMPI-PES) investigations.[11] Multichannel quantum defect theory (MQDT) calculations based on such studies have ultimately led to a characterization of the autoionizing Rydberg states between the $^2\Pi_{3/2}$ and $^2\Pi_{1/2}$ ionic limits.[4,5]

The important conclusion that rotational and spin–orbit interactions are dominantly responsible for the dynamic properties of these states implies that studies of such states under conditions where one or both of these interactions is considerably different would be of interest. It is in this spirit that we have initiated an extensive study of the autoionizing Rydberg states in HBr, where spin–orbit coupling is considerably larger. Moreover, analysis of the autoionizing region is simplified since the lowest autoionizing Rydberg states already occur for $n=7$, while in HCl a crowded spectrum has been obtained starting at $n=14$.[2,4,5]

Although for HBr the spectroscopic constants of the $X\ ^2\Pi$ ionic ground state are well known,[12] the lowest ionization threshold has only been determined with relatively low resolution techniques.[13,14] In the present study we have determined the lowest ionization threshold and investigated the role of discrete–discrete and discrete–continuum interactions by REMPI-PES and ZEKE-PFI techniques via the $f\ ^3\Delta_2$ and $F\ ^1\Delta_2$ Rydberg states. The electronic configuration of the $f\ ^3\Delta_2$ and $F\ ^1\Delta_2$ Rydberg states of HBr consists of a $5p\pi$ Rydberg electron coupled to a $(\sigma^2\pi^3)^2\Pi$ ionic core. Due to the strong spin–orbit coupling the observable states are a 1:1 mixture of $^1\Delta_2$ and $^3\Delta_2$. As explained in Ref. 15 one can consider the $f\ ^3\Delta_2$ state to be built upon the $^2\Pi_{3/2}$ ionic core and the $F\ ^1\Delta_2$ state on the $^2\Pi_{1/2}$ ionic core. Although it is clear that formally both states should be described in Hund's case (c), we will continue to label the states in Hund's case (a) in order to avoid confusion with the notation of previous studies, which employed Hund's case (a) labeling as well. The experimental results will be compared with the results of *ab initio* calculations.

II. EXPERIMENTAL DETAILS

The ZEKE-PFI setup employed in our experiments has been described before.[11] Only the main features will be reiterated. The heart of the setup consists of a ''magnetic bottle'' spectrometer, on whose pole faces two grids have been installed for application of static and pulsed electric fields. In the current ZEKE-PFI experiments the 2 mm gap between the two grids defines the ionization region. The grid (2 mm hole diameter) nearest to the flight tube is grounded, while at the other grid a variable negative bias is applied, usually in the order of -0.2 to -0.5 V. After a certain time delay this voltage is switched to a value which can be varied between -0.4 V to -5 V, corresponding to electric fields of 2–25 V/cm. The time delays possible in the present experiments vary from 30 ns to 500 ns, which is considerably shorter than those utilized in most other ZEKE-PFI experiments. The reason for this difference is found in the observation that the ZEKE-PFI signal decreases drastically after about 100 ns. This is ascribed mainly to the drifting of molecules in high-n Rydberg states out of the ionization region. The ZEKE-PFI spectra to be presented have been obtained with a delay of 60 ns.

For comparison with the ZEKE-PFI results, dispersive photoelectron measurements have also been performed. One color $2+1$ REMPI via the intermediate Rydberg state produced photoelectrons that were subsequently analyzed according to their kinetic energies. The resulting energies correspond to the various quantum states of the ion reached in the REMPI process. In these REMPI-PES experiments a resolution of 10 meV could be realized, as compared to 0.5 meV possible in our setup when using the ZEKE-PFI technique.

The experiments were performed using a Lumonics HyperEX 400 excimer laser pumping two Lumonics dye lasers (HD500 and HD300), both operating on Coumarin 500. Fundamental light from one of the dye lasers was frequency-doubled using a BBO crystal. This linearly polarized light was then focused into the ionization region by a quartz lens with a focal length of 25 mm and was used to pump various electronically excited rovibronic levels of HBr. The fundamental output from the other dye laser was focused by a separate lens on the opposite side of the spectrometer and was scanned over the various ionization thresholds of the $^2\Pi_{3/2}$ or the $^2\Pi_{1/2}$ ionic states. Both laser pulses were overlapped in time using a fast silicon photodiode (HP 5082). Both the fundamental and UV output of the dye lasers intersected an effusive beam of pure HBr (Messer Griesheim 2.8, 99.8%) in the ionization region.

The pump and probe dye lasers were calibrated using a neon optogalvanic lamp.[16] Additional calibrations of the dye lasers were performed by employing known HBr (Ref. 17) and Xe (Ref. 18) $2+1$ REMPI resonances. The resulting accuracy of the dye lasers is estimated to be about 0.5 cm^{-1}.

III. RESULTS AND DISCUSSION

A. Ionization limit

Before we discuss how the lowest ionization threshold of HBr is determined, we must first consider the issue of stray fields in our spectrometer. Usually ZEKE spectrometers are built such that local electric stray fields are kept to a minimum by applying electric as well as magnetic shielding. Such an approach is not possible with a ''magnetic bottle'' spectrometer. As a result there are not only unknown stray electric fields present, but the molecule will also experience a motional Stark field proportional to **vxB**,[19] in which the velocity of the molecule is represented by **v** and the magnetic field by **B**. Worst case estimates of this field indicate that it may have a magnitude as large as 3 V/cm in our experiments on HBr.[20] These stray fields present a problem if one wishes to derive a field-free ionization limit. In the following two independent methods for an accurate determination of the ionization energy (IE) will be discussed. In the first technique, which is not a ZEKE method, the threshold is determined in such a way that the stray fields can be neglected. In the second method not only the IE is determined, but also the combined magnitude of our stray fields is derived.

In the first approach the onset of ionization is measured as a function of an applied dc electric field which is much larger than any stray fields present, and subsequently extrapolated to zero field. The applied fields range from 500 V/cm down to 25 V/cm. The onset of ionization can then be obtained from the well known square-root dependence $\mathrm{IE}(E) = \mathrm{IE}(0) - C\sqrt{E}$, where E is the applied electric field in V/cm and C a proportionality constant.[20]

The field-free value of the $^2\Pi_{3/2}$ ionization limit has been determined using the intermediate $f\,^3\Delta_2$ ($v'=0$, $J'=2$) Rydberg state excited via the $R(1)$ rotational two-photon transition. Subsequently one photon of the probe laser is absorbed, which is scanned across the ionization threshold. The onset of ionization (FWHM 3 cm^{-1}) was determined as a function of the applied electric field. A least-squares fit according to the above equation resulted in a C-factor equal to 4.96 ± 0.05, a value that is somewhat lower than the theoretical result of ≈ 6.[20] However, deviations from this value have been observed before.[21,22] Ionization thresholds were also measured for electric fields smaller than 25 V/cm but were found to be strongly nonlinear with respect to the square-root dependence. This nonlinearity is attributed mainly to the unknown contribution of stray fields, although contributions from collisional ionization under low field conditions may be also present.[23] Using the described technique the field-free ionization limit of HBr $[X\,^1\Sigma^+(v''=0,\ J''=0) \rightarrow X\,^2\Pi_{3/2}(v^+=0,\ J^+=3/2)]$ is found to be $94\,098.7 \pm 1$ cm^{-1}. We note that this value of the ionization limit is in excellent agreement with the IE obtained by Irrgang *et al.*, $94\,099.8 \pm 2$ cm^{-1}, in a one-photon VUV ZEKE-PFI study.[24]

To verify this result, a second method was employed. In this case HBr is seeded with xenon. The ZEKE-PFI method is then applied to xenon under the same experimental conditions used for HBr, i.e., using a 1 V/cm bias and a 2 V/cm extraction pulse resulting in a 3.5 cm^{-1} FWHM ZEKE-

resolution, although the laser power was reduced considerably to avoid ac Stark shifts. The first laser is fixed on the xenon $6p[5/2]_2$ two-photon resonance,[18] while the second laser scans the $^2P_{3/2}$ ionic limit. Since the $^2P_{3/2}$ limit of xenon is well known,[18] we are able to evaluate the deviation of the ionic limit from the literature value. This difference is due to the combination of the applied dc and pulsed electric fields, and any stray fields present in the spectrometer. In this way the total shift from the true ionization limit was found to be 7.0 ± 1.0 cm^{-1}, of which the applied dc and pulsed field contribute 5.3 cm^{-1}. The dc contribution was obtained by measuring the ionization limit with a bias of zero, while the contribution of the pulsed electric field was taken as the FWHM value of the ZEKE-PFI signal. The remaining shift of 1.7 cm^{-1} is purely due to the stray fields which are estimated to be around 0.1 V/cm, assuming a *C*-factor of 5. The magnitude of this stray field has been verified using other xenon resonances as well. It is surprising, but at the same time gratifying to find that this stray field is considerably smaller than the worst case estimate of 3 V/cm mentioned above. These results therefore indicate that the influence of the magnetic field is not as large as previously feared and show that accurate ZEKE-PFI measurements can indeed be performed in a ''magnetic bottle'' spectrometer.

The motional Stark field is velocity- and thus mass-dependent. This implies that the measured ionization threshold of HBr formally cannot be corrected directly with the 7.0 cm^{-1} obtained from the ZEKE-PFI measurements on xenon. However, assuming that the deduced stray field of 0.1 V/cm is entirely due to the motional Stark effect, we calculate that the maximum motional Stark shift in HBr would be 1.8 cm^{-1} as opposed to 1.7 cm^{-1} found for xenon. The difference of 0.1 cm^{-1} is well within the accuracy of our experiments, and we have therefore applied the correction of 7.0 cm^{-1} to obtain an IE for HBr of $94\,098.9\pm1$ cm^{-1}. The observation that this value is within the accuracy of the result derived in the threshold extrapolation method supports our assumption that we can use the same correction for xenon and HBr. The rotational and upper spin–orbit thresholds are then calculated using accurately known spectroscopic constants obtained by Lubic *et al.*[12] and compare very well with the measured values. These results are given in Table I.

TABLE I. Rotational thresholds of the $^2\Pi_{3/2}$ and $^2\Pi_{1/2}$ ionic states. The uncertainty in the $^2\Pi_{3/2}$ and $^2\Pi_{1/2}$ rotational thresholds is 1 and 3 cm^{-1}, respectively.

Ionic rotational level	$^2\Pi_{3/2}$ thresholds[a] (cm^{-1})	$^2\Pi_{3/2}$ thresholds[b] (cm^{-1})	$^2\Pi_{1/2}$ thresholds[a] (cm^{-1})	$^2\Pi_{1/2}$ thresholds[c] (cm^{-1})
+1/2			96 741.6	96 741.6[d]
−1/2			96 743.6	96 743.6[d]
+3/2	94 098.9	94 098.9	96 768.6	96 767.8
−3/2			96 764.5	96 765.4
+5/2	94 138.6	94 138.6	96 803.4	96 803.3
−5/2			96 809.5	96 809.0
+7/2	94 194.0	94 193.9	96 866.2	96 865.4
−7/2			96 858.1	96 859.0
+9/2	94 265.3	94 265.0	96 928.8	96 929.7
−9/2			96 938.9	96 938.0
+11/2	94 352.4	94 352.2	97 027.5	97 027.5
−11/2			97 015.3	97 015.4
+13/2	94 455.1	94 454.9	97 177.6	97 117.0
−13/2			97 131.8	97 130.6
+15/2	94 573.5	94 573.5	97 251.9	97 250.9
−15/2			97 235.7	97 235.1

[a]Calculated rotational levels based upon spectroscopic constants from Lubic *et al.* (Ref. 12) relative to the $J^+=3/2(^2\Pi_{3/2})$ ionization threshold as determined from experimental spectra.
[b]Rotational levels obtained from experimental spectra.
[c]Levels derived by measurement of the rotational thresholds with respect to the $J^+=1/2(^2\Pi_{1/2})$ rotational threshold (see comment d).
[d]Rotational level derived using the experimentally obtained $J^+=3/2(^2\Pi_{3/2})$ threshold in combination with the spin–orbit constant from Lubic *et al.* (Ref. 12).

B. REMPI-PES

Figure 1(a) depicts a rotationally resolved photoelectron spectrum deriving from one-color (2+1) REMPI via the $S(9)$ rotational transition of the $f\,^3\Delta_2$ ($v'=0$, $J'=11$) Rydberg state of HBr. The figure shows that ionization takes place to the ground vibrational level of the ion, and that only the $^2\Pi_{3/2}$ spin–orbit component is populated in the photoionization process. We notice that core preservation in HBr is stronger than in HCl, where it was observed that the spin–orbit ratio $^2\Pi_{3/2}$:$^2\Pi_{1/2}$ for ionization via the corresponding Rydberg state is 6:1.[11] Rotationally resolved photoelectron spectroscopy becomes possible when the instrumental resolution exceeds the ionic rotational spacing. For HCl this occurs via a lower J' than for HBr, since the ionic state rotational constant is somewhat larger in HCl (9.788 cm^{-1} vs 7.956 cm^{-1}). Figure 1(a) shows that ionization of HBr via the $f\,^3\Delta_2(v'=0,\ J'=11)$ rotational level occurs predominantly with $\Delta J=J^+-J'=+1/2$, and that $\Delta J>0$ transitions are considerably more intense than those with $\Delta J<0$.

One-photon ionization of the $f\,^3\Delta_2$ Rydberg state occurs under the restriction of a number of selection rules. First, conservation of total angular momentum requires that the only allowed transitions are those for which $|\Delta J|\leqslant l+3/2$,[25] in which l is the orbital angular momentum associated with the partial wave component of the photoelectron. Secondly, in a Hund's case (a) description the parity, p, of the final ionic rotational levels should conform to the selection rule[25] $\Delta J+\Delta S+\Delta p+l=$even, where $\Delta p=p^+-p'$, and $p=0$ for e states and 1 for f states. On the basis of the angular momentum composition of the $5p\pi$ orbital of the $f\,^3\Delta_2$ Rydberg state [95.56% p, 4.33% d, 0.06% f, and 0.02% g (Ref. 26)] one-photon ionization of this state would consequently be expected to lead to photoelectrons with predominantly s and d partial wave components. Under these assumptions the dominant transitions in the photoelectron spectrum should be those for $|\Delta J|\leqslant 7/2$ and will be associated with a change in parity.

For the photoelectron spectrum depicted in Fig. 1(a), excitation from the ground state to the $f\,^3\Delta_2(v'=0)$ state via the $S(9)$ rotational transition populates only the $J'=11$ negative parity component. Assuming predominantly s and d partial wave components for the photoelectron, photoionization

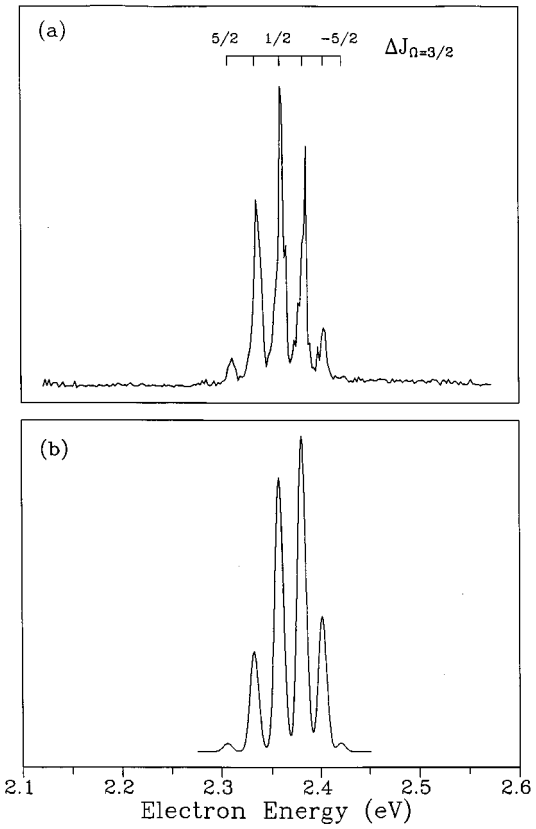

FIG. 1. REMPI-PES spectrum associated with the $f\ ^3\Delta_2$ ($v'=0$) Rydberg state via the $S(9)$ rotational transition. (a) Experimental spectrum and (b) its corresponding simulation (alignment included).

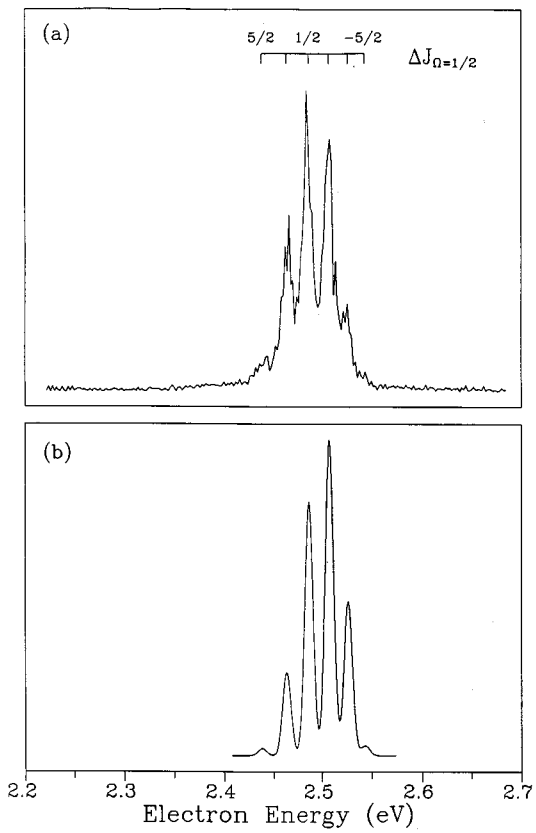

FIG. 2. REMPI-PES spectrum associated with the $F\ ^1\Delta_2$ ($v'=0$) Rydberg state via the $Q(10)$ rotational transition. (a) Experimental spectrum and (b) its corresponding simulation (alignment included).

should lead primarily to a population of positive parity ionic rotational levels. However, each rotational level of the $^2\Pi_{3/2}$ ionic state consists of a positive and negative parity component, and since the lambda doubling is extremely small (<0.1 cm^{-1}),[12] we are unable to determine experimentally which parity is favored in the photoionization process.

Figure 1(b) shows the simulation of the photoelectron spectrum via the same intermediate level. All calculations presented in this work were carried out using theoretical and computational procedures discussed previously in Ref. 9, using the parameters defined in Wang and McKoy.[26] It is observed that the $\Delta J=-1/2$ transition is the most intense, though only slightly more so than the $\Delta J=+1/2$ transition. More importantly, however, is that in the calculation an almost equal intensity is predicted for the $\Delta J<0$ transitions and their $\Delta J>0$ counterparts, which is contrary to our experimental observations.

Figure 2(a) shows the photoelectron spectrum obtained for ionization via the $Q(10)$ transition of the $F\ ^1\Delta_2(v'=0)$ Rydberg state. Again, only the $\Delta v=0$ transition is observed and ionization occurs with total core preservation. The ionic rotational distribution is very similar to that observed for ionization via the $f\ ^3\Delta_2$ state; $\Delta J=+1/2$ is the dominant transition, and $\Delta J>0$ transitions are more intense than those with $\Delta J<0$.

Similar to the one-photon ionization process from the $f\ ^3\Delta_2(v'=0)$ Rydberg state, the angular momentum composition of the Rydberg electron of the $F\ ^1\Delta_2(v'=0)$ Rydberg state [96.57% p, 3.39% d, and 0.03% f (Ref. 26)] would lead one to expect an ionization process from this state with dominant s and d partial waves, limiting $|\Delta J|$ to 7/2. Lambda doubling in the $^2\Pi_{1/2}$ ionic state is much larger than in the $^2\Pi_{3/2}$ state; for $J^+=1/2$ the splitting between the e and f levels is ≈ 2 cm^{-1} and approximately another 2 cm^{-1} is added for each successive J^+.[12] Hence, it might become possible to identify which parity of the ionic rotational level is favored on photoionization, despite the fact that the widths of the peaks in the photoelectron spectrum are ≈ 80 cm^{-1}. The excitation route via $Q(10)$ accesses the positive parity component of the $J'=10$ rotational level, which implies that negative parity ionic rotational levels would be expected to be dominant in the photoelectron spectrum if even partial waves dominate the photoionization process.

The calculated photoelectron spectrum for ionization via the $F\ ^1\Delta_2(v'=0)$ $Q(10)$ transition is depicted in Fig. 2(b). The $\Delta J=-1/2$ transition is predicted to be the most intense one, contrary to the experimental result. At odds with the experiment is also that in the calculations $\Delta J<0$ transitions have a larger intensity than the $\Delta J>0$ ones. The discrepancies are, however, less pronounced than for the $f\ ^3\Delta_2$ calcu-

lation. Finally, it is interesting to note that the REMPI-PES spectra measured for HBr via the $F\ ^1\Delta_2$ and $f\ ^3\Delta_2$ states are very similar to those of HCl recorded by De Beer *et al.* via the same states.[11] Both measurements reveal that the transition with $\Delta J=+1/2$ is dominant.[27]

C. ZEKE-PFI

Figures 3(a) and 3(b) show a series of ZEKE-PFI spectra to the $^2\Pi_{3/2}$ rotational ionic limits measured via the S and P rotational branches of the $f\ ^3\Delta_2(v'=0,\ J'=2-7)$ Rydberg state, respectively. The ZEKE-PFI spectra via $J'=2-5$ were recorded with an extraction pulse of 2 V/cm. Since the intensity of the ZEKE-PFI signal decreased for excitation of higher J', spectra via $J'=6-7$ were measured using a 10 V/cm pulse. In order to ascertain that the rotational branching ratios do not change upon increasing the pulsed electric field, spectra obtained via excitation of lower J' levels were also measured using the 10 V/cm extraction pulse. As expected, no significant intensity differences are observed with the spectra obtained with the 2 V/cm pulse, although the width of the ZEKE-PFI peaks is considerably larger when an electric field pulse of 10 V/cm is employed.

Figures 3(a) and 3(b) show that in all the ZEKE-PFI spectra measured via either the P or S rotational branches of the $f\ ^3\Delta_2$ Rydberg state transitions with $\Delta J<0$ are more intense than those with $\Delta J>0$. This is opposite to what is observed in REMPI-PES. Considering excitations via $S(0)$ to $S(3)$ and via $P(3)$ to $P(6)$ in Figs. 3(a) and 3(b) the most intense features in the spectra are transitions to $J^+=3/2$. Another observation is that as we proceed via higher J' the intensity distribution gradually shifts to higher J^+. On excitation via $S(4)$ and higher members of the S branch the most intense rotational transition is no longer to $J^+=3/2$. Assuming that the ejected electron has strong d partial wave character, the allowed rotational transitions in the ZEKE-PFI spectra are $|\Delta J|\leqslant 7/2$. This implies that when exciting via the $S(4)$ [or $P(7)$] and $S(5)$ [or $P(8)$] rotational transitions, the $J^+=3/2$ and $J^+=3/2$, 5/2 respectively, levels must be due to $l=3$ or higher waves and hence can be expected to be weak.

In Figs. 3(a) and 3(b) the theoretical simulations of the ZEKE-PFI spectra are shown as well. Since lambda doubling cannot be resolved for the $^2\Pi_{3/2}$ ionic state, the intensities for both parities have been added in the simulations. The calculations show that transitions with $\Delta J<0$ are slightly more intense than those with $\Delta J>0$, except for excitation via the $S(0)$ rotational transition. The agreement between theory and experiment when exciting via the lowest J' is quite good and less so for excitation via higher J'.

Figures 4(a) and 4(b) show ZEKE-PFI spectra measured in the region of the $^2\Pi_{1/2}$ ionic state threshold via the S and R rotational branches of the $F\ ^1\Delta_2$ $(v'=0,\ J'=2-6)$ Rydberg state. Again, $\Delta J<0$ transitions are more intense than their $\Delta J>0$ counterparts. The allowed rotational transitions (assuming s and d partial waves) have the same restriction on ΔJ as for the $f\ ^3\Delta_2$ state. However, similar to the ZEKE-PFI spectra via the $f\ ^3\Delta_2$ state, we are observing ΔJ transitions on excitation via the $S(3)$ [or $R(4)$] and $S(4)$ [or $R(5)$] rotational transitions which should nominally be forbidden. In the ZEKE-PFI via the $f\ ^3\Delta_2$ state we observed that the transition to the lowest ionic rotational level $(J^+=3/2)$ was dominant in all the spectra up to $J'=5$. Here, this dominance is reduced considerably: the transition to the lowest ionic rotational level of the $^2\Pi_{1/2}$ state $(J^+=1/2)$ only dominates for $J'=2$ and 3.

The ZEKE-PFI signal for ionization via the $F\ ^1\Delta_2$ state was considerably smaller than that observed via the $f\ ^3\Delta_2$ state, and hence a larger extraction pulse (10 V/cm) was employed, causing a significant broadening of the ZEKE-PFI lines. Despite this broadening the lambda doubling of the $^2\Pi_{1/2}$ ionic state is resolved. On excitation via lower J' levels, the parity components of the ionic rotational level cannot be resolved, but as we progress to higher J' both parity components can be seen, although (depending on J') one parity component is still dominant. Excitation of a particular J' rotational level in the intermediate state via the S or R rotational branch leads to the population of different parity components in the intermediate state. In agreement with the experimental results of Figs. 4(a) and 4(b), and results of previous studies,[26] the subsequent ionization step gives rise to population in different parity components in the ionic manifold.

If we assume that the dominant partial wave is even, then ionization via the $S(0)$ rotational transition of the $F\ ^1\Delta_2$ state should favor the negative parities of the $^2\Pi_{1/2}$ ionic rotational levels. Via the $S(1)$ transition, positive parities are preferred, and so on. Figures 4(a) and 4(b) confirm that even partial waves are dominant. However, if one examines the spectra more closely, contributions from odd partial waves are present as well. The presence of odd partial waves is more evident at higher J^+, where their intensities become comparable to the even partial wave contributions. Similar observations have been made by Xie and Zare.[26] Clearly, the photoionization dynamics are not strictly atomiclike.

The calculations of the ZEKE-PFI spectra via the $F\ ^1\Delta_2$ Rydberg state are depicted in Figs. 4(a) and 4(b) as well. Since lambda doubling for the $^2\Pi_{1/2}$ ionic state can easily be resolved, the contributions from the two parties have been treated separately in the calculations. Comparison of the simulated spectra with the experimental results shows that when excitation takes place via the lowest rotational transition, i.e., $S(0)$ or $R(1)$, the agreement is quite good, but gets poorer as we progress via higher J'.

To obtain a qualitative understanding of the differences observed between the REMPI-PES and ZEKE-PFI spectra, it is necessary to explicitly take the effects of autoionization into consideration.[10,11,29] In our ZEKE-PFI experiments our primary aim is to populate high-n Rydberg states converging upon a certain rotational threshold J^+ of the ionic manifold. At the same time, however, low-n Rydberg states converging upon higher J^+ rotational levels, which can coincidentally be almost degenerate with the high-n Rydberg states, can be-

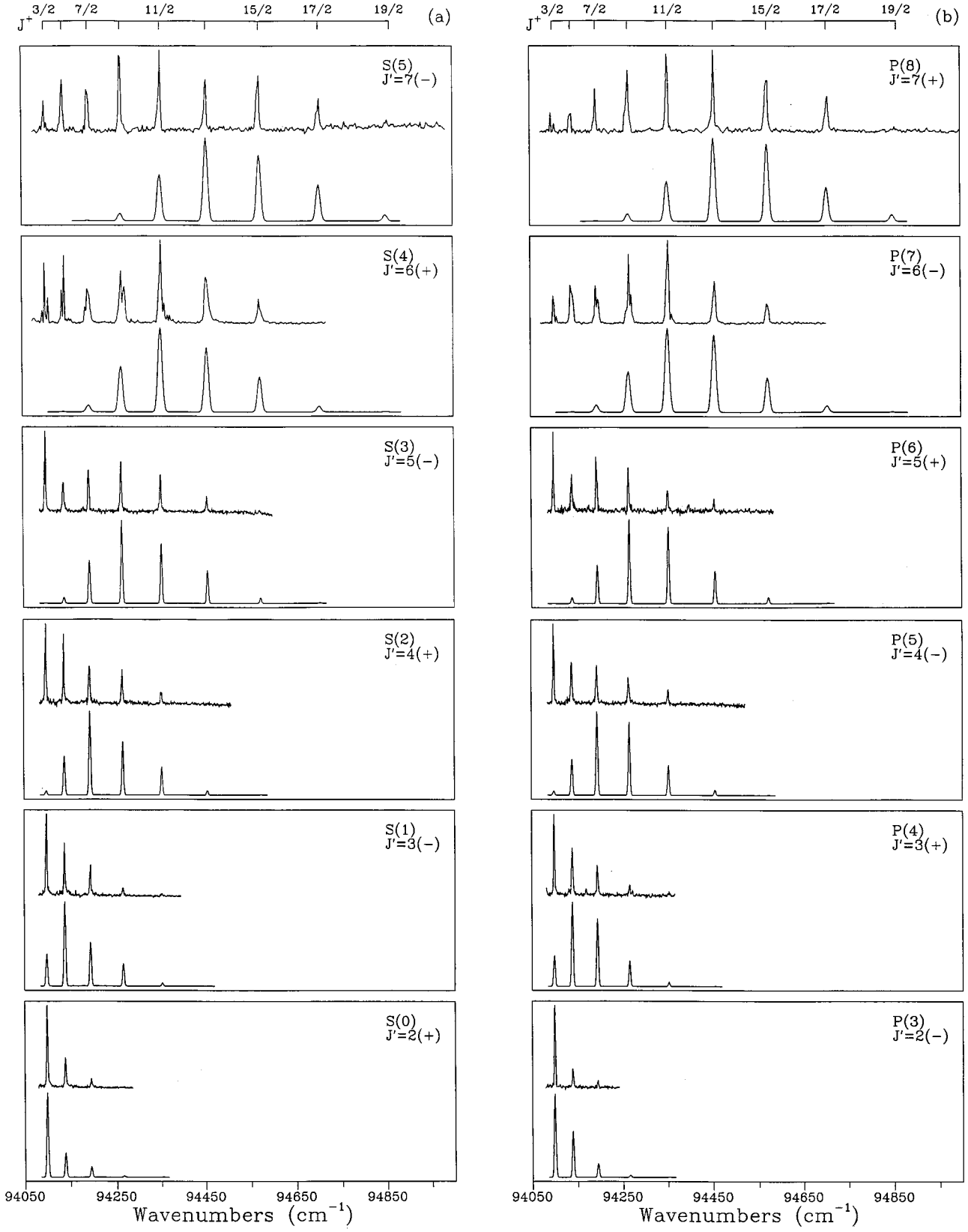

FIG. 3. ZEKE-PFI spectra associated with the $f\,^3\Delta_2$ ($v'=0$) Rydberg state via (a) the S and (b) P rotational branches. The top spectra represent the experimental spectra, the bottom ones the simulated spectra (alignment included). Transitions via higher values of J' are fitted with a 10 cm^{-1} Gaussian line form. The sign between the brackets indicates the parity of the level.

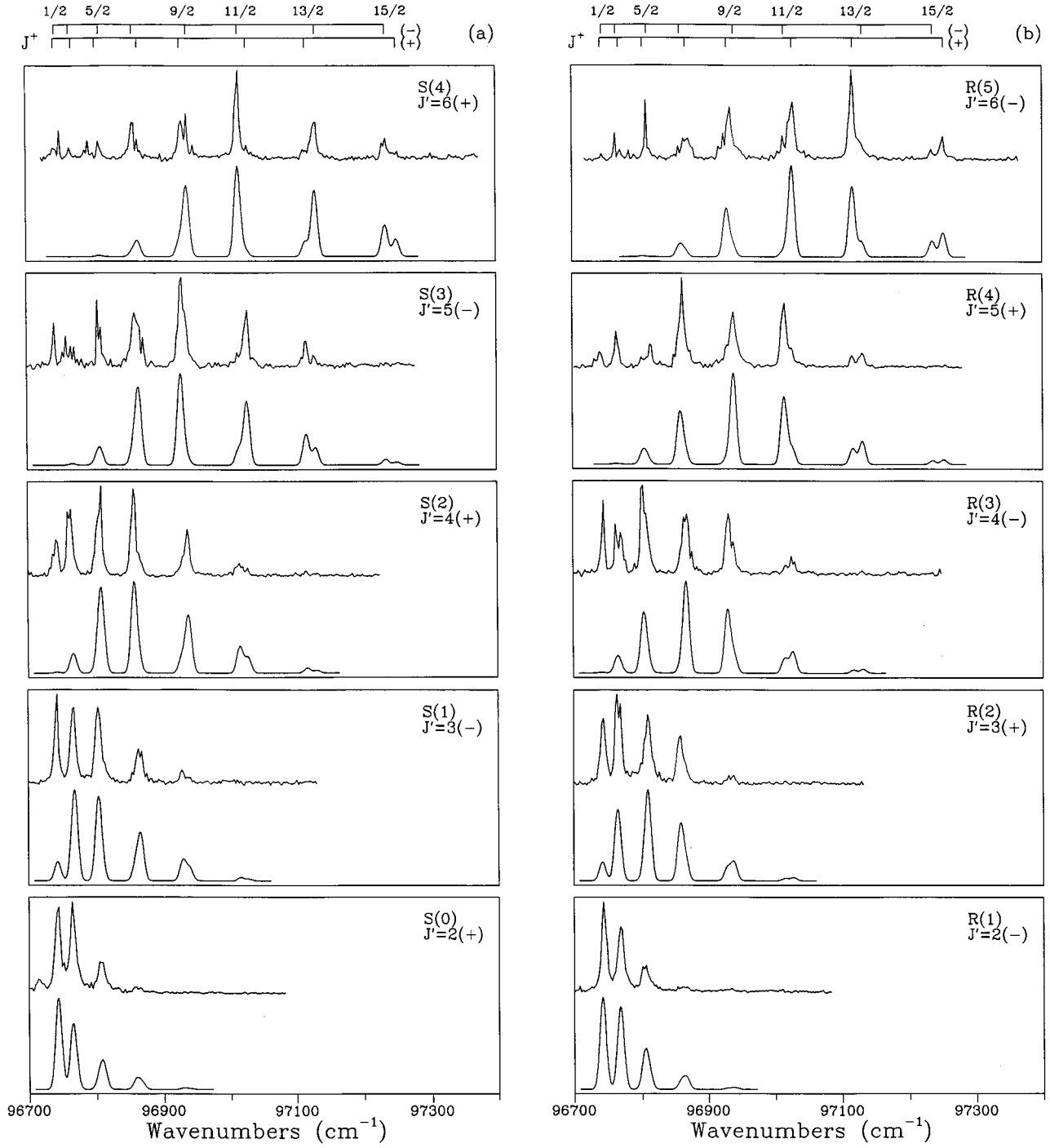

FIG. 4. ZEKE-PFI spectra associated with the $F\,^1\Delta_2$ ($v'=0$) Rydberg state via (a) the *S* and (b) *R* rotational branches. The top spectra represent the experimental spectra, the bottom ones the simulated spectra (alignment included). The simulation is convoluted using a 10 cm^{-1} FWHM Gaussian line form. The sign between the brackets indicates the parity of the level.

come populated. These low-*n* Rydberg states may couple via rotational and/or spin–orbit interactions to the high-*n* Rydberg states. When the pulsed field is switched on, the ionization continua associated with the rotational threshold of the high-*n* Rydberg states will consequently also become available to the low-*n* Rydberg states, resulting in an increase in the observed intensity of the J^+ level to which the high-*n* Rydberg states belong. Since the number of low-*n* Rydberg states that can possibly be excited is higher for $\Delta J<0$ transitions than for their $\Delta J>0$ counterparts, $\Delta J<0$ transitions in general gain more intensity than $\Delta J>0$ transitions.[10]

The above mechanism implies that the Rydberg states involved in the pulsed field ionization to the $J^+=3/2$ ($^2\Pi_{3/2}$) and $J^+=1/2$ ($^2\Pi_{1/2}$) rotational thresholds are rather unique. The former states can only decay through mechanisms other than autoionization, viz., radiation or predissociation. So, in

contrast to the situation for the higher J^+ levels of the $^2\Pi_{3/2}$ ionic state, the $J^+=3/2$ ZEKE-PFI signal can only be enhanced through ''forced'' autoionization, which in this case is limited to rotational autoionization. This is supported by the observation in Fig. 3 that the $J^+=3/2$ ($^2\Pi_{3/2}$) ZEKE-PFI signal is so dominant in the spectra up to $J'=5$. For transitions via higher values of J', ionization to the $J^+=3/2$ ionic rotational level is no longer allowed, assuming *s* and *d* partial waves, and accordingly much lower intensities are observed. The situation is slightly different for the Rydberg states converging upon the $J^+=1/2$ ($^2\Pi_{1/2}$) ionic level. Although these states are not subject to rotational autoionization, they might autoionize via spin–orbit coupling, which would lead to a population depletion of the J^+ levels of the $^2\Pi_{1/2}$ state in general. Indeed, it has been observed that in HCl such a mechanism is of dominant importance, and leads to a completely different $^2\Pi_{3/2}$:$^2\Pi_{1/2}$ branching ratio than observed via REMPI-PES.[11] However, setting aside this mechanism of spin–orbit autoionization, it is clear that at the $J^+=1/2$ ($^2\Pi_{1/2}$) rotational threshold the situation resembles to a large extent that at the $J^+=3/2$ ($^2\Pi_{3/2}$) ionic threshold; once again the $J^+=1/2$ ZEKE-PFI signal can only be enhanced by rotational autoionization.

When only transitions with $\Delta J \geqslant 1/2$ are compared, we see that in most ZEKE-PFI spectra the simulations show approximate agreement with experiment. This is in line with our previous reasoning, since at higher J^+ rotational thresholds discrete–discrete interactions, which enhance the ZEKE-PFI intensity at lower J^+ rotational thresholds, are moderated. Such a conclusion has also been reached by Zhu *et al.*[9] who concluded that simulations of ZEKE-PFI spectra of HCl could be well compared with experimental results if the lowest ionic rotational level was excluded.

We notice that the anomalies in the rotational branching ratios can be explained by an increase of the ZEKE-PFI signal intensities by the above processes of ''forced'' rotational and spin–orbit autoionization. Recently, another explanation has been proposed which is based on a population loss of high-*n* Rydberg states due to rotational and spin–orbit autoionization during the delay period before the pulsed field is switched on.[30,31] In this mechanism intensity perturbations result from the different autoionization decay rates of Rydberg states converging upon the various spin–orbit and rotational thresholds. Studies of CO_2 (Ref. 30) and, in particular, HCl (Ref. 32) have unequivocally shown that such a mechanism is at least in part responsible for the differences between experimental and theoretical results. It is, however, not capable of explaining the large intensities of ''forbidden'' transitions in the ZEKE-PFI spectra.

In HCl a comparison between the spin–orbit components has been made for ZEKE-PFI via the $f\ ^3\Delta_2$ and $F\ ^1\Delta_2$ Rydberg states.[11] For the $F\ ^1\Delta_2$ state it was observed that in the photoelectron spectrum the $^2\Pi_{1/2}$ core dominated, as expected, while in the corresponding ZEKE-PFI spectrum the $^2\Pi_{3/2}$ ionic core was the most intense. The $f\ ^3\Delta_2$ state, on the other hand, displayed similar spin–orbit ratios in both the photoelectron and ZEKE-PFI spectra. This was rationalized in that Rydberg states converging upon the $^2\Pi_{1/2}$ ionic state were subject to spin–orbit autoionization, thereby diminishing the ZEKE-PFI signal and at the same time increasing the signal in the lower spin-substate.[11] Such a direct comparison between the relative intensities of the two spin–orbit components is difficult in the case of HBr, due to the large spin–orbit splitting of some 2500 cm^{-1} in the $X\ ^2\Pi$ ionic state. Our REMPI-PES spectra have shown that the $F\ ^1\Delta_2$ state is a Rydberg state with a very pure ionic core ($^2\Pi_{1/2}$). Accordingly, we would be led to believe that ZEKE-PFI spectroscopy in the region of the $^2\Pi_{3/2}$ ionic limit would not lead to observable transitions, since excitation of high-*n* Rydberg states converging upon its rotational thresholds would be largely forbidden. In contrast to these *a priori* expectations, ZEKE-PFI spectroscopy in this region did show discernible transitions. The resonances in these spectra did, however, not exhibit the line shapes as observed for the majority of the resonances in Figs. 3 and 4, but showed a sharp substructure. Moreover, in a number of cases resonances were even missing where, on the basis of the presence of neighboring resonances, they would have been expected to be present. These observations can be rationalized when we realize that the resonances that we see in fact derive from very low-*n* Rydberg states converging upon $^2\Pi_{1/2}$ ionic rotational thresholds. Indeed, two-color REMPI-PES experiments, in which we have investigated the autoionizing resonances between the $^2\Pi_{3/2}$ and $^2\Pi_{1/2}$ states in HBr, reveal that the energies of the resonances observed in the ZEKE-PFI experiments coincide with the energies of such autoionizing resonances.[33] We therefore conclude that spin–orbit autoionization still may play an important role in HBr. Such a conclusion is in line with our observation that the ZEKE-PFI signals via the $F\ ^1\Delta_2$ state in the region of the $^2\Pi_{1/2}$ limit are considerably less intense than those obtained after excitation of the $f\ ^3\Delta_2$ state in the region of the $^2\Pi_{3/2}$ limit.

Our observation of sharp-structured ZEKE-PFI peaks is similar to what has been observed in previous studies on NO_2 and HI.[34,35] In these molecules, however, the basis of the structure was found in rotational interactions, due to which interlopers converging upon higher rotational thresholds became apparent. Evidence for these rotational interactions, apart from their evident influence on the rotational branching ratios, is also found in our ZEKE-PFI spectra, in particular when a larger amplitude of the pulsed field is employed. The spectra obtained after excitation of the $F\ ^1\Delta_2$ state via the $S(3)$ and $S(4)$ transitions are clear examples where the sharp structure observed near the $J^+=1/2$ and 3/2 thresholds can only be accounted for by Rydberg states converging upon higher rotational limits.

As mentioned before, forbidden transitions were observed in the experimental ZEKE-PFI spectra (see Figs. 3 and 4). The fact that we are able to observe them indicates that there are higher *l* components present in the outgoing wave of the ejected Rydberg electron. Although the calculations show that the angular composition of the $F\ ^1\Delta_2$ and $f\ ^3\Delta_2$ states of HBr have predominantly *p* character, higher *l* contributions are present as well. This result indicates that the outgoing wave of the ejected electron is composed not

only of *s* and *d* (even) partial waves, but of also some *p* and *f* (odd) partial waves. The *f* partial wave permits larger changes in rotational angular momentum, and hence the ''forbidden'' transitions become slightly allowed. Indeed such transitions are evident in the REMPI-PES spectra.

The arguments presented above indicate that a detailed theoretical analysis and prediction of the ZEKE-PFI spectra of HBr require that relevant interactions responsible for the observed effects of autoionization are explicitly taken into account. It is therefore not surprising that the simulations shown in Figs. 3 and 4 deviate considerably from the experimental spectra.

IV. CONCLUSIONS

The combined application of REMPI-PES and ZEKE-PFI spectroscopy via the $f\,^3\Delta_2$ and $F\,^1\Delta_2$ Rydberg states of HBr allows for a detailed investigation of the photoionization dynamics of low- and high-*n* Rydberg states in HBr, and for an accurate determination of the lowest ionization threshold as $94\,098.9\pm1\ \mathrm{cm}^{-1}$. Photoionization dynamics of the $f\,^3\Delta_2$ and $F\,^1\Delta_2$ Rydberg states as probed by dispersive REMPI-PES show that these states carry the signature of ionization of a *p* electron. Interestingly, however, the comparison with the results of *ab initio* calculations reveals significant discrepancies with respect to the rotational branching ratios upon ionization. ZEKE-PFI spectroscopy after excitation of these two Rydberg states, on the other hand, shows rotational branching ratios indicative of a dominant role of discrete–discrete and/or discrete–continuum interactions during the delay period in this type of experiment. The differences between theoretical calculations and experimental results are shown to appear most prominently for $\Delta J<1/2$ transitions, while rotational intensities for $\Delta J\geqslant1/2$ transitions indicate, at least qualitatively, a reasonable agreement. A quantitative analysis of ZEKE-PFI spectra would consequently benefit considerably from calculations, which not only take the static electronic properties of initial and final states into account, but also the dynamic evolution of the high-*n* Rydberg states involved in the PFI process.

ACKNOWLEDGMENTS

N.P.L.W. thanks R. Irrgang for communicating his ZEKE-PFI results prior to publication. The group at the University of Amsterdam gratefully acknowledges the Netherlands Organization for Scientific Research (NWO) for equipment grants and for financial support. Calculations performed by H.L.B. have used the French National Computer (CNUSC). The Amsterdam and Pasedena groups gratefully acknowledge NATO for collaborative Grant No. CRG930183. Work at the California Institute of Technology was supported by the Air Force Office of Scientific Research, the Office of Health and Environmental Research of the U.S. Department of Energy, and made use of the JPL/Caltech CRAY Y-MP2E/232 computer.

[1] H. Lefebvre-Brion, P. M. Dehmer, and W. A. Chupka, J. Chem. Phys. **85**, 45 (1986).
[2] K. S. Haber, E. Patsilinakou, Y. Jiang, and E. R. Grant, J. Chem. Phys. **94**, 3429 (1991).
[3] A. Mank, M. Drescher, T. Huth-Fehre, N. Böwering, U. Heinzmann, and H. Lefebvre-Brion, J. Chem. Phys. **95**, 1676 (1991).
[4] Y.-F. Zhu, E. R. Grant, and H. Lefebvre-Brion, J. Chem. Phys. **99**, 2287 (1993).
[5] M. Drescher, A. Brockhinke, N. Böwering, U. Heinzmann, and H. Lefebvre-Brion, J. Chem. Phys. **99**, 2300 (1993).
[6] H. Lefebvre-Brion, J. Chem. Phys. **93**, 5898 (1990).
[7] K. Müller-Dethlefs and E. W. Schlag, Annu. Rev. Phys. Chem. **42**, 109 (1991).
[8] K. G. Lubic, D. Ray, D. C. Hovde, L. Veseth, and R. J. Saykally, J. Mol. Spectrosc. **134**, 1 (1989).
[9] Y.-F. Zhu, E. R. Grant, K. Wang, V. McKoy, and H. Lefebvre-Brion, J. Chem. Phys. **100**, 8633 (1994).
[10] R. G. Tonkyn, R. T. Wiedmann, and M. G. White, J. Chem. Phys. **96**, 3696 (1992).
[11] E. de Beer, W. J. Buma, and C. A. de Lange, J. Chem. Phys. **99**, 3252 (1993).
[12] K. G. Lubic, D. Ray, D. C. Hovde, L. Veseth, and R. J. Saykally, J. Mol. Spectrosc. **134**, 21 (1989).
[13] D. A. Shaw, D. Cvejanovic, G. C. King, and F. H. Read, J. Phys. B **17**, 1173 (1984).
[14] B. Ruscic and J. Berkowitz, J. Chem. Phys. **93**, 1747 (1990).
[15] H. Lefebvre-Brion, Chem. Phys. Lett. **171**, 377 (1990).
[16] *CRC Handbook of Chemistry and Physics*, 66th ed. edited by R. C. Weast (Chemical Rubber, Boca Raton, 1985–1986), p. E-259.
[17] R. Callaghan and R. J. Gordon, J. Chem. Phys. **93**, 4624 (1990).
[18] C. E. Moore, Natl. Bur. Stand (U.S.) Circ. 35 (1971), Vol. III, p. 113.
[19] C. W. Clark, K. T. Lu, and A. F. Starace, in *Progress in Atomic Spectroscopy (Part C)*, edited by H. J. Beyer and H. Kleinpoppen (Plenum, New York, 1984).
[20] W. A. Chupka, J. Chem. Phys. **98**, 4520 (1993).
[21] T. Ebata, Y. Anezaki, M. Fujii, N. Mikami, and M. Ito, J. Phys. Chem. **87**, 4773 (1983).
[22] S. T. Pratt, J. Chem. Phys. **98**, 9241 (1993).
[23] L. A. Chewter, M. Sander, K. Müller-Dethlefs, and E. W. Schlag, J. Chem. Phys. **86**, 4737 (1987).
[24] R. Irrgang, M. Drescher, F. Gierschner, M. Spieweck, and U. Heinzmann, J. Electron. Spectrosc. Relat. Phenom. (in press).
[25] J. Xie and R. N. Zare, J. Chem. Phys. **93**, 3033 (1990); K. Wang and V. McKoy, J. Chem. Phys. **95**, 4977 (1991); S. N. Dixit and V. McKoy, Chem. Phys. Lett. **128**, 49 (1986); G. Raseev and N. Cherepkov, Phys. Rev. A **42**, 3948 (1990).
[26] K. Wang and V. McKoy, J. Chem. Phys. **95**, 7872 (1991).
[27] As the result of the small lambda splitting in the $^2\Pi_{1/2}$ ionic state no unambiguous assignment was made in Ref. 11. A reanalysis of the results shows, however, that the maximum of the photoelectron spectrum via the $S(8)$ rotational transition to the $F\,^1\Delta_2$ state of HCl should be the $\Delta J=+1/2$ transition and not the $\Delta J=-1/2$ transition.
[28] J. Xie and R. N. Zare, Chem. Phys. Lett. **159**, 399 (1989).
[29] K. S. Haber, Yanan Jiang, Gregg Bryant, E. R. Grant, and H. Lefebvre-Brion, Phys. Rev. A **44**, R5331 (1991).
[30] R. T. Wiedmann, M. G. White, H. Lefebvre-Brion, and C. Cossart-Magos, J. Chem. Phys. **103**, 10417 (1995).
[31] H. Lefebvre-Brion, Chem. Phys. Lett. (submitted).
[32] N. P. L. Wales, W. J. Buma, and C. A. de Lange (unpublished).
[33] N. P. L. Wales, W. J. Buma, C. A. de Lange, and H. Lefebvre-Brion (in preparation).
[34] G. P. Bryant, Y. Jiang, M. Martin, and E. R. Grant, J. Chem. Phys. **101**, 7199 (1994).
[35] S. T. Pratt, J. Chem. Phys. **101**, 8302 (1994).